Z-scan measurements of the anisotropy of nonlinear refraction and absorption in crystals

R. DeSalvo, M. Sheik-Bahae, A. A. Said, D. J. Hagan, and E. W. Van Stryland

Center for Research in Electro-Optics and Lasers, University of Central Florida, Orlando, Florida 32816

Received September 21, 1992

We introduce a method for measuring the anisotropy of nonlinear absorption and nonlinear refraction in crystals by incorporating a wave plate into the Z-scan apparatus. We demonstrate this method by measuring the polarization dependence of the nonlinear refractive index or two-photon absorption coefficient in BaF_2, KTP, and GaAs at wavelengths of 532 and 1064 nm.

The techniques most often used to determine components of the third-order susceptibility, $\chi^{(3)}$, include degenerate four-wave mixing,[1] nearly degenerate three- and four-wave mixing,[2] ellipse rotation,[3] optical third-harmonic generation,[4] photoacoustics,[5] beam-distortion methods,[6-8] and nonlinear transmission.[9] Some of these have been adapted to measure the anisotropy of $\chi^{(3)}$.[2,5,6,9] We introduce a method based on the Z-scan[8,10] to determine the polarization dependence of nonlinear refraction and nonlinear absorption in crystals. We demonstrate this technique to measure anisotropy of the ultrafast bound electronic nonlinear refractive index n_2 and the two-photon absorption (2PA) coefficient β. Measurements of the anisotropy can also give information about the band structure of the material.[11] Sheik-Bahae *et al.*[8] describe the Z scan in detail, where the transmittance of a sample is measured through an aperture in the far field as a function of the sample's position relative to the beam waist. If only nonlinear refraction is present, a transmittance curve, with a maximum (peak) and a minimum (valley), antisymmetric around the position of the beam waist is obtained. The peak-to-valley change in transmittance, ΔT_{pv}, is approximately proportional to the on-axis nonlinear phase shift $\Delta\Phi_o$.[8] It is shown that $\Delta T_{pv} \simeq p|\Delta\Phi_o| = pk|\Delta n|L$, where k is the propagation vector and L is the length of the sample. The constant p depends on the size of the aperture in the far field and equals 0.36 for an aperture allowing 40% linear transmittance. Placing the sample at the Z position corresponding to the peak, a half-wave plate situated in front of the sample is rotated, and the transmittance through the aperture is measured as a function of the incident linear polarization direction. This is repeated with the sample positioned at the valley. By subtracting these two sets of data, we obtain ΔT_{pv} as a function of incident electric-field polarization, from which we can infer the polarization dependence of n_2. Here we define n_2 by the change in refractive index, $\Delta n = n_2 I$.

When the aperture is removed and all the transmitted energy is collected, the experiment is sensitive only to changes in transmittance due to the presence of nonlinear absorption. When the sample is placed at the beam waist, the loss is maximized, and rotation of the wave plate shows the anisotropy of this loss. To normalize the transmittance change and eliminate other small polarization-dependent losses, a second measurement is performed, with the sample placed far from the waist such that the nonlinear loss is negligible. Subtraction of these data from the data with the sample at the waist gives the normalized transmittance change through the sample, and hence the 2PA coefficient β can be calculated from a spatial and temporal integration of the equation

$$\frac{\partial I(r,z',t)}{\partial z'} = -\alpha I(r,z',t) - \beta I(r,z',t)^2, \qquad (1)$$

where z' is the depth in the sample and α is the residual linear absorption coefficient.[12] Measurement of the anisotropy of n_2 in the presence of nonlinear absorption requires a more complicated procedure.[8]

Following Ref. 13, given an input field $E(t) = E_o \cos(\omega t)$, the amplitude of the third-order polarization at ω is given by

$$P^{(3)}(\omega) = \frac{3\epsilon_o}{4}\chi_{\text{eff}}^{(3)}(\theta)E_o{}^3, \qquad (2)$$

where ϵ_o is the dielectric permittivity and $\chi_{\text{eff}}^{(3)}$ is the effective third-order susceptibility whose functional form depends on the symmetry and orientation of the crystal. The intensity-dependent refractive index n_2 and the 2PA coefficient β are related to the real and imaginary parts of $\chi^{(3)}$ by[8]

$$n_2\,(\text{m}^2/\text{W}) = \frac{3}{4\epsilon_o c n_o{}^2}\text{Re}\,\chi^{(3)}(\omega;-\omega,\omega,\omega) \qquad (3)$$

and

$$\beta\,(\text{m/W}) = \frac{3\omega}{2\epsilon_o c^2 n_o{}^2}\text{Im}\,\chi^{(3)}(\omega;-\omega,\omega,\omega), \qquad (4)$$

where n_o is the linear refractive index and c is the speed of light in a vacuum. We use mks units throughout, and the conventions used here follow those of Ref. 14. The conversion to esu is $n_2^{\text{esu}} = (cn_o/40\pi)n_2^{\text{mks}}$, where $\Delta n = n_2^{\text{esu}}E_o{}^2/2$.

The Q-switched mode-locked Nd:YAG laser used for these experiments produced single 30-ps (FWHM)

0146-9592/93/030194-03$5.00/0

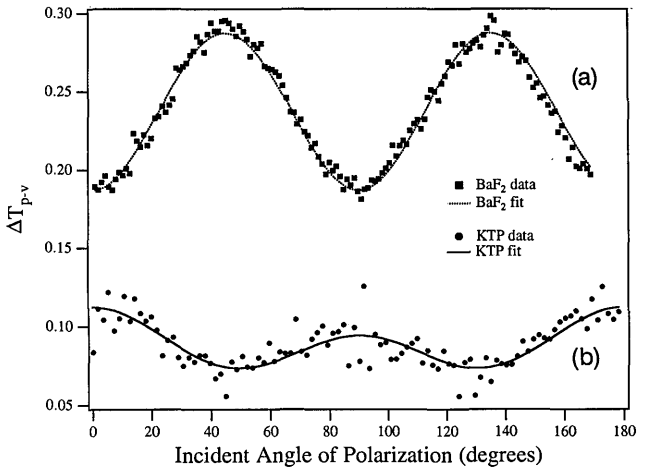

Fig. 1. Curve (a), 532-mn 40% aperture transmittance trace as a function of incident electric-field polarization in BaF_2. Curve (b), 1064-nm trace in KTP to measure the polarization dependence of n_2.

TEM_{00}-mode pulses that could be frequency doubled to obtain 21-ps 532-nm pulses. When using 1064-nm pulses, we focused the beam to a measured spot size of 37 μm (half-width at $1/e^2$ maximum) with a best-form lens, whereas at 532 nm, the beam waist was 24 μm.

Looking first at BaF_2, which has a cubic lattice belonging to the point group $m3m$, we define the electric-field polarization direction θ relative to the [100] crystallographic axis and propagate $\mathbf{k}$ parallel to the [001] crystallographic axis. Figure 1, curve (a), shows data of the aperture transmittance versus polarization orientation of n_2 at 532 nm with an irradiance of 61 GW/cm^2 for a 0.5-cm-thick sample of BaF_2. The electric-field polarization in the crystallographic xy plane is given by $\mathbf{E} = E_o(\cos\theta\hat{x} + \sin\theta\hat{y})$. Because we consider degenerate frequencies, intrinsic permutation symmetry leaves three independent $\chi^{(3)}$ tensor components given by $\chi^{(3)}_{xxxx}$, $\chi^{(3)}_{xyyx}$, and $\chi^{(3)}_{xxyy}$. Note that this is true for both real and imaginary parts of $\chi^{(3)}$. For this specific geometry, the effective third-order susceptibility from Eq. (2) is

$$\chi^{(3)}_{\text{eff}}(\theta) = \chi^{(3)}_{xxxx}[1 + 2\sigma(\sin^4\theta - \sin^2\theta)], \qquad (5)$$

where we define a coefficient of anisotropy σ as

$$\sigma = \frac{\chi^{(3)}_{xxxx} - \left[\chi^{(3)}_{xxyy} + 2\chi^{(3)}_{xyyx}\right]}{\chi^{(3)}_{xxxx}}. \qquad (6)$$

If the material is isotropic, i.e., $\chi^{(3)}_{xxxx} = \chi^{(3)}_{xxyy} + 2\chi^{(3)}_{xyyx}$, σ yields a value of zero. The dashed curve in Fig. 1 is a least-squares fit to Eq. (5) with only real components of $\chi^{(3)}$. The values of the nonlinear coefficients for BaF_2 and other materials are summarized in Table 1, where the absolute errors are $\pm 20\%$.

For z-cut KTP, which has an orthorhombic lattice and belongs to the point group $mm2$, we propagate $\mathbf{k}$ along the crystal's z axis so that the electric-field polarization will be in the xy plane making an angle ϕ with the crystallographic x axis. In this geometry, $d_{\text{eff}} = 0$ for both type I and type II phase matching[15]; thus, quasi-$\chi^{(3)}$ effects that are due to cascading of second-order processes[16] are eliminated, and the nonlinearity is purely bound electronic and positive.[16] Applying intrinsic permutation symmetry, we arrive at an effective third-order susceptibility,

$$\chi^{(3)}_{\text{eff}}(\phi) = \chi^{(3)}_{xxxx}\cos^4\phi + \chi^{(3)}_{yyyy}\sin^4\phi + B\frac{\sin^2 2\phi}{4}, \qquad (7)$$

where B is given by

$$B = 2\chi^{(3)}_{xxyy} + 2\chi^{(3)}_{yyxx} + \chi^{(3)}_{xyyx} + \chi^{(3)}_{yxxy}. \qquad (8)$$

Figure 1, curve (b), shows the aperture transmittance versus ϕ at 1064 nm in a 0.76-mm sample of KTP with an irradiance of 46 GW/cm^2. The least-squares fit to Eq. (7) is shown as the solid curve in Fig. 1.

At 532 nm, KTP exhibits 2PA. The solid curve and dots in Fig. 2 show the transmittance versus ϕ with the aperture removed and the sample at the beam waist for an irradiance of 32 GW/cm^2. The solid curve in Fig. 2 is a least-squares fit of Eq. (7).

GaAs is a $\bar{4}3m$ cubic material and shows 2PA at 1064 nm. The GaAs sample was oriented so that $\mathbf{k}$ was normal to the [110] plane, and the electric-field polarization was measured relative to the [001] crystallographic axis. The dotted curve and crosses in Fig. 2 show the transmittance versus polarization angle θ in a 0.8-mm sample placed at the beam waist with an irradiance of 180 MW/cm^2. Following the analysis for cubic BaF_2, we find that

$$\chi^{(3)}_{\text{eff}}(\theta) = \chi^{(3)}_{xxxx}\left[1 + 2\sigma\left(\frac{3}{4}\sin^4\theta - \sin^2\theta\right)\right]. \qquad (9)$$

In contrast to the case of BaF_2, only the imaginary components of $\chi^{(3)}$ are used in evaluating Eqs. (6) and (9). The least-squares fit to the data is shown as the dashed curve in Fig. 2. The value of the anisotropy of β reported here agrees well with that reported by Bepko,[9] using nanosecond pulses, where 2PA-generated carrier absorption is large and simply

Table 1. Summary of Nonlinear Coefficients n_2 and β Measured at 532 and 1064 nm

BaF_2	$\text{Re}[\chi^{(3)}_{xxxx}]$ (m^2/V^2)	σ	n_2(m^2/W)[100]	n_2(m^2/W)[010]	n_2(m^2/W)[110]	
532 nm	1.59×10^{-22}	-1.08 ± 0.10	2.08×10^{-20}	2.08×10^{-20}	3.22×10^{-20}	
GaAs	$\text{Im}[\chi^{(3)}_{xxxx}]$ (m^2/V^2)	σ	β(cm/GW)[100]	β(cm/GW)[110]	β(cm/GW)[111]	
1064 nm	6.35×10^{-19}	-0.74 ± 0.18	18	24	25	
KTP	$\text{Re}[\chi^{(3)}_{xxxx}]$ (m^2/V^2)	$\text{Re}[\chi^{(3)}_{yyyy}]$ (m^2/V^2)	Re(B)(m^2/V^2)	n_2(m^2/W)[100]	n_2(m^2/W)[010]	n_2(m^2/W)[110]
1064 nm	23.2×10^{-22}	19.6×10^{-22}	18.5×10^{-22}	21.4×10^{-20}	18.1×10^{-20}	13.9×10^{-22}
KTP	$\text{Im}[\chi^{(3)}_{xxxx}]$ (m^2/V^2)	$\text{Im}[\chi^{(3)}_{yyyy}]$ (m^2/V^2)	Im(B)(m^2/V^2)	β(cm/GW)[100]	β(cm/GW)[010]	β(cm/GW)[110]
532 nm	11.7×10^{-22}	7.77×10^{-22}	3.96×10^{-22}	0.24	0.16	0.14

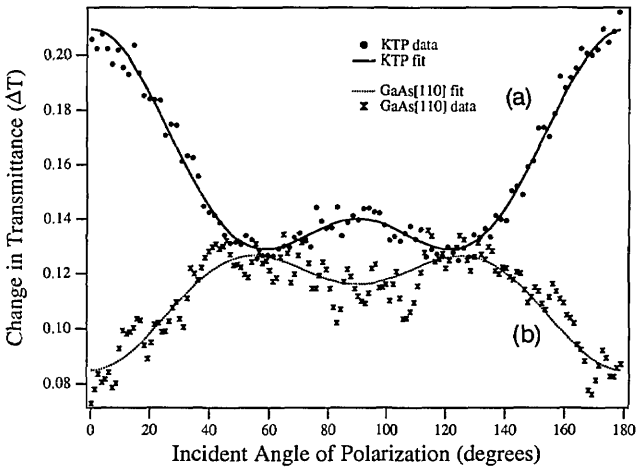

Fig. 2. Curve (a), 532-nm data for KTP showing variation in change in transmittance as a function of incident polarization. Curve (b), 1064-nm trace in [110] GaAs showing variation in transmittance as a function of incident electric-field polarization.

reflects the anisotropic nature of the band structure. The same value of anisotropy has been theoretically predicted[17] and subsequently measured[18] for the real part of $\chi^{(3)}$ at a wavelength of 10.6 μm.

Use of wave-plate rotation rather than repeated Z scans at different electric-field polarization orientations keeps the sample stationary, thus minimizing any beam walk at the aperture, and hence increasing the sensitivity for measuring the anisotropy. By choosing specific crystal orientations and wave-vector propagation directions, different third-order tensor susceptibility elements can be determined.

We gratefully acknowledge the support of the National Science Foundation (Grant ECS-9120590), the Defense Advanced Research Projects Agency/Night Vision and Electro Optics Directorate, and the Florida High Technology and Industrial Council. In addition, we thank Brian Wherrett of Heriot-Watt University for helpful discussions, R. Adair of Lawrence Livermore National Laboratories for supplying the BaF_2 sample, G. Witt of the Massachusetts Institute of Technology for the GaAs sample, and Bruce Chai for determining crystal orientations.

D. J. Hagan is also with the Department of Physics, University of Central Florida.

E. W. Van Stryland is also with the Department of Physics and Electrical Engineering, University of Central Florida.

References

1. E. J. Canto-Said, D. J. Hagan, J. Young, and E. W. Van Stryland, IEEE J. Quantum Electron. **27,** 2274 (1991).
2. R. Adair, L. L. Chase, and S. A. Payne, Phys. Rev. B **39,** 3337 (1989).
3. A. Owyoung, IEEE J. Quantum Electron. **QE-11,** 1064 (1973).
4. P. D. Maker and R. W. Terhune, Phys. Rev. **137,** A801 (1965).
5. Y. Bae, J. J. Song, and Y. B. Kim, J. Appl. Phys. **53,** 615 (1982).
6. A. A. Borshch, M. S. Brodin, and V. N. Semioshko, Phys. Status Solidi A **91,** 135 (1985).
7. W. E. Williams, M. J. Soileau, and E. W. Van Stryland, in *Fifteenth Annual Symposium on Optical Materials for High Power Lasers* (National Bureau of Standards, Washington, D.C., 1983).
8. M. Sheik-Bahae, A. A. Said, T. H. Wei, D. J. Hagan, and E. W. Van Stryland, IEEE J. Quantum Electron **26,** 760 (1990).
9. S. J. Bepko, Phys. Rev. B **12,** 669 (1975).
10. J. R. DeSalvo, D. J. Hagan, M. Sheik-Bahae, and E. W. Van Stryland, in *Optical Society of America Annual Meeting Technical Digest* (Optical Society of America, Washington, D.C., 1990), paper MTT7.
11. S. I. Shablaev, Sov. Phys. JETP **70,** 1105 (1990).
12. A. A. Said, M. Sheik-Bahae, D. J. Hagan, T. H. Wei, J. Wang, J. Young, and E. W. Van Stryland, J. Opt. Soc. Am. B **9,** 405 (1992).
13. P. N. Butcher and D. Cotter, *Elements of Nonlinear Optics* (Cambridge U. Press, London, 1990), Chap. 2.
14. D. C. Hutchings, M. Sheik-Bahae, D. J. Hagan, and E. W. Van Stryland, Opt. Quantum Electron. **24,** 1 (1992).
15. T. Yee Fan, C. E. Huang, B. Q. Hu, R. C. Echardt, Y. X. Fan, R. L. Byer, and R. S. Feigelson, Appl. Opt. **26,** 2390 (1987).
16. R. DeSalvo, D. J. Hagan, M. Sheik-Bahae, G. I. Stegeman, E. W. Van Stryland, and H. Vanherzeele, Opt. Lett. **17,** 28 (1992).
17. C. Flytzanis, Phys. Lett. **31A,** 273 (1970).
18. E. Yablonovitch, C. Flytzanis, and N. Bloembergen, Phys. Rev. Lett. **29,** 865 (1972).